

FLC based Modular Multilevel converter for an Induction Motor

T. Penchalaiah¹, S. Vijay², G. Sridhar Babu³, A. Mano Ranjith Kumar⁴

¹⁻⁴EEE Department, ^{1&3}St. Martin's Engineering College, Dhulapally, ²Bharath Institute of Engineering & Technology, Ibrahimptnam, ⁴Global College of Engineering, Chennai

¹smec.penchal99@gmail.com, ²svijay0416@gmail.com, ³sridharbabueee@smec.ac.in,

⁴manoranjith015@gmail.com

Abstract— This paper presents theoretical and simulation discussions on a practical speed- Sensor-less start-up method for an induction motor driven by a modular multilevel cascade inverter based on double-star chopper cells (MMCI-DSCC) from standstill to middle speed using fuzzy controller. This motor drive is suitable, particularly for a large-capacity fan- or blower-like load. The load torque is proportional to a square of the motor mechanical speed. The start-up method is characterized by combining capacitor-voltage control with motor-speed control. The motor-speed control with the minimal stator current plays a crucial role in eliminating a speed sensor from the drive system and in reducing an ac voltage fluctuation occurring across each dc capacitor. Several start-up waveforms show stable performance from standstill to middle speed with different load torques. Simulation waveforms can be verified by using MATLAB/SIMULINK.

Keywords— Induction Motor Drives, Multilevel Converter Modular multilevel converter (MMC), Fuzzy logic controller (FLC).

I. INTRODUCTION

Attention has been paid to medium-voltage motor drives for energy savings without regenerative brakes [1]–[4]. A modular multilevel cascade inverter based on double star chopper cells (MMCI-DSCC) has been expected as one of the next-generation medium- voltage multilevel pulse width modulation (PWM) inverters for such motor drives [5]–[14]. For the sake of simplicity, the MMCI-DSCC is referred to as the “DSCC” in this paper [5]. Each leg of the DSCC consists of two positive and negative arms and a center-tapped inductor sitting between the two arms. Each arm consists of multiple bidirectional dc/dc choppers called as “chopper cells.” The low voltage sides of the chopper cells are connected in cascade, while the electrically floating high-voltage sides of chopper cells are equipped with a dc capacitor and a voltage sensor. A synergy effect of lower voltage steps and phase-shifted PWM leads to lower harmonic voltage and current, as well as lower EMI emission, as the count of cascaded chopper cells per leg increases. The power conversion circuit of the DSCC is so flexible in design that any count of cascaded chopper cells is theoretically possible [6]. When a DSCC is applied to an ac motor drive, the DSCC would suffer from ac-voltage fluctuations in the dc-capacitor voltages of each chopper cell in a low-speed range, because the ac-voltage fluctuation gets more serious as a stator-current frequency gets lower [7]. Hence, the fluctuation should be attenuated satisfactorily to achieve stable low-speed and start-up performance. Several papers have exclusively discussed startup methods for DSCC-based induction motor drives [10]–[14]. The authors in [10] proposed a simple start-up method with no speed sensor, in which a DSCC continued to be operated at an appropriate constant frequency, e.g., 30 Hz, to reduce the ac-voltage fluctuation during the start-up. Here, the ac output voltage was adjusted appropriately to produce a required startup torque. However, an over current may flow not only in the DSCC but also in the motor because a slip frequency in a low speed range get much higher than the rated slip-frequency. This results in producing a reduced motor torque.

Other start-up methods from standstill were discussed for DSCC-driven induction motors, where each of the motors was equipped with a speed sensor. A serious ac-voltage fluctuation in a low-speed range can be mitigated by injecting a common-mode voltage and superimposing a circulating current on each leg of the DSCC. Generally, it is desirable to eliminate a speed sensor from a motor drive, particularly when a motor drive is introduced to a hostile environment when a new DSCC is applied to an already-existing line-started motor with no speed sensor, or when a long lead cable is required to connect a new DSCC with a new motor.

The aim of this paper is to verify the effectiveness and practicability of a speed-Sensor-less start-up method for a DSCC based induction motor drive, in which the motor starts rotating from standstill to middle speed with a ramp change. This motor drive is suitable, particularly for an application to a fan- or blower-like load. The load torque is proportional to a square of the motor mechanical speed and is changing slow enough to be considered as steady-state conditions. The start-up method discussed in this paper is characterized by combining capacitor voltage control with motor-speed control. The capacitor-voltage control plays a part in regulating the mean dc voltage of each of the dc capacitors [7] and in mitigating the ac voltage appearing across

each dc capacitor, which fluctuates at the stator-current frequency [4], [14]. The motor- speed control makes it possible to eliminate a speed sensor from the drive system and to mitigate the ac- voltage fluctuation in all the frequency range. This motor-speed control relies on an equivalent circuit of an induction motor, which was proposed in [17]. It is somewhat similar in basic idea to conventional “volts-per-hertz” or shortly “V/f” and “slip- frequency” control techniques, but different in terms of combining the two control techniques together. The motor-speed control is based on “feedback” control of the stator current, which is the same as that in the slip-frequency control, whereas the commands for the amplitude and frequency of the stator current are based on “feed forward” control in consideration of a speed-versus-load-torque characteristic, as done in the V/f control. Therefore, neither motor parameter nor speed sensor is required. Furthermore, the motor- speed control is applicable to any inverter equipped with current sensors at the ac terminals. As a result, the start-up torque is enhanced by a factor of three, without additional stress on arm currents and dc- capacitor voltages. Several start-up waveforms show stable performance from standstill to middle speed with different load torques.

II. CIRCUIT CONFIGURATION AND CAPACITOR-VOLTAGE CONTROL OF THE DSCC

A. Circuit Configuration

Fig. 1(a) shows the main circuit configuration of the DSCC discussed in this paper. Each leg consists of eight cascaded bidirectional chopper cells shown in Fig. 1(b) and a center tapped inductor per phase, as shown in Fig. 1(c). The center tap of each inductor is connected directly to each of the stator terminals of an induction motor, where it is the u-phase stator current. The center-tapped inductor is more cost effective than two non coupled inductors per leg, because the center tapped inductor presents inductance LZ only to the circulating current iZ and no inductance to the stator current iu [7]. It brings significant reductions in size, weight, and cost of the magnetic core.1 These advantages in the center- tapped inductor are mostly welcomed, particularly applications to motor drives, in which no ac inductors are required between the motor and the inverter. In Fig. 1, instantaneous currents iPu and iNu are the u phase positive- and negative-arm currents, respectively, and iZu is the u-phase circulating current defined as follows [7]:

$$i_{Zu} \triangleq \frac{1}{2}(i_{Pu} + i_{Nu}) \tag{1}$$

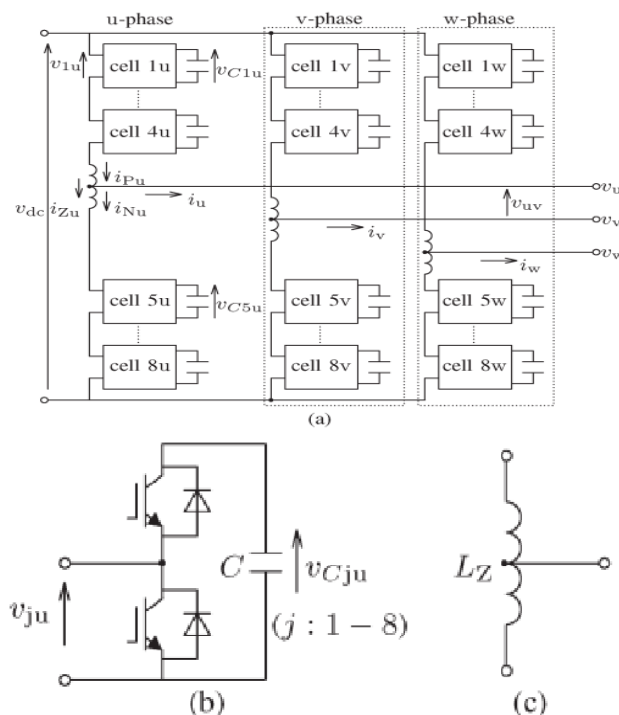


Fig.1. Circuit configuration for an MMCI-DSCC. (a) Power circuit. (b) Chopper cell. (c) Center-tapped inductor.

Note that iZu includes dc and ac components to be used for the capacitor-voltage control. The dc component flows from the common dc link to each leg, while the ac component circulates among the three legs. The individual ac components included in the three-phase circulating currents $\tilde{i}_{Zu}, \tilde{i}_{Zv}$, and \tilde{i}_{Zw} cancel each other out, so that no ac component appears in either motor current or dc-link current.

The arm currents i_{Pu} and i_{Nu} can be expressed as linear functions of two independent variables i_u and i_{Zu} as follows [7]:

$$i_{Pu} = \frac{i_u}{2} + i_{Zu} \tag{2}$$

$$i_{Nu} = -\frac{i_u}{2} + i_{Zu} \tag{3}$$

The dc-capacitor voltage in each chopper cell consists of dc and ac components causing an ac- voltage fluctuation. When neither common-mode voltage nor ac circulating current is Superimposed, the peak-to-peak ac-voltage fluctuation Δv_{Cju} is approximated as follows [10]:

$$\Delta v_{Cju} \approx \frac{\sqrt{2}I_1}{4\pi f c} \tag{4}$$

Where I_1 is the rms value of the stator current, f is the frequency of the stator current, and C is the capacitance value of each dc capacitor. According to (4), Δv_{Cju} is inversely proportional to f and proportional to I_1 . Hence, Δv_{Cju} increases as the stator-current frequency decreases.

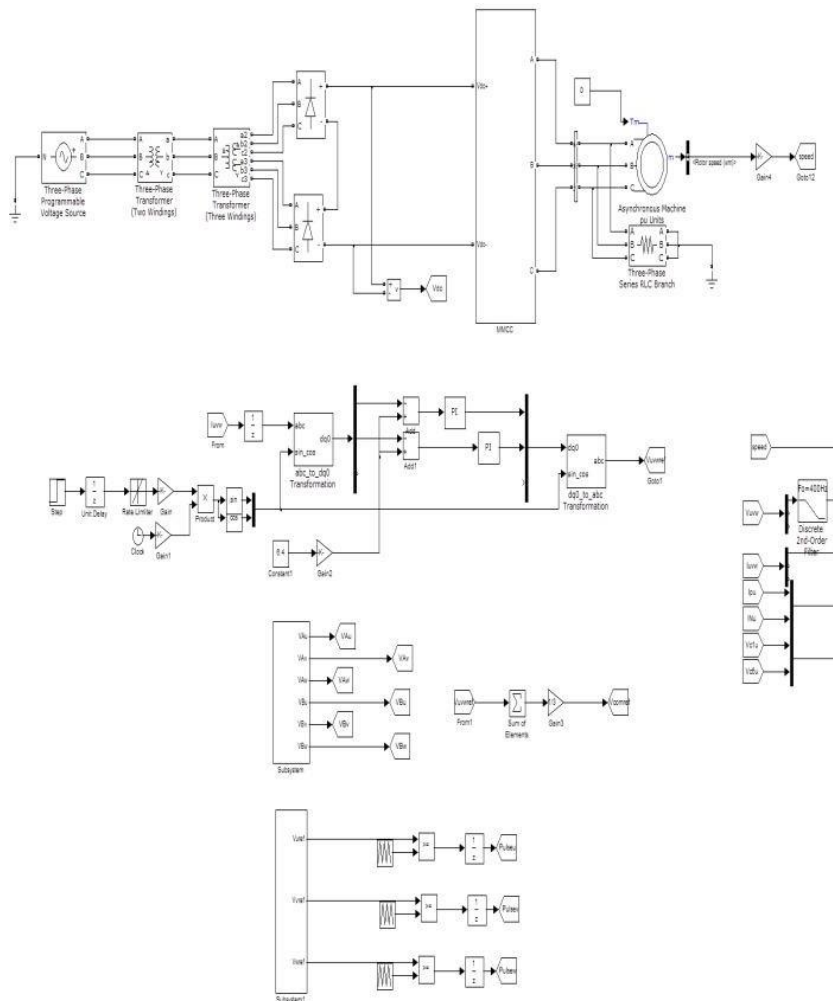


Fig. 2. Overall control block diagram

Increases the ac-voltage fluctuation is undesirable due to the following reasons

- It affects the voltage rating of insulated-gate bipolar transistors.
- It causes over modulation to each chopper cell.
- It makes the system unstable because the ac-voltage fluctuation can be considered as a disturbance to the control system.

Therefore, the ac-voltage fluctuation should be mitigated to an acceptable level

B. Capacitor-Voltage Control

Fig. 2 shows the overall control block diagram of the startup method. The 24 dc-capacitor voltages v_{Cjvw} , the dc-link voltage v_{dc} , and the six arm currents i_{Puvw} and i_{Nuvw} are detected, and they are input signals for the block diagram. Note that the three stator currents i_{uvw} are calculated from the detected arm currents. This paper employs two kinds of existing capacitor-voltage control techniques for regulating the mean dc voltage of each dc capacitor and for mitigating the ac-voltage fluctuation at the stator-current frequency. The mean dc-voltage regulation can be achieved by using the “arm” balancing control applied to the six arms and the “individual” balancing control applied to the one arm at the same time [7]. The ac-voltage fluctuation can be mitigated by the sophisticated control discussed in [13]. This control interacts the common-mode voltage v_{com} , which is injected to three center-tap terminals of the DSCC with the ac components of the three circulating currents \tilde{i}_{Zuvw} . This can mitigate the ac voltage fluctuation at the stator-current frequency, thus leading to start up from standstill. As a result, the remaining ac-voltage fluctuations are independent of the time-varying frequencies of the stator current, but dependent on a fixed frequency of the injected common-mode voltage (50 Hz in this experiment). The circulating current feedback control included in the mean dc voltage regulation block yields a command voltage of v_a^* .

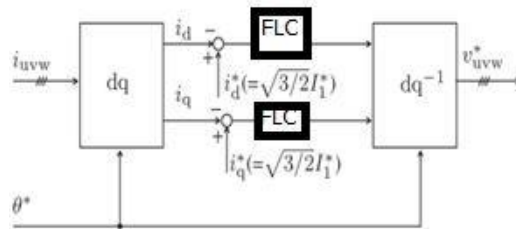


Fig.3. Block diagram of speed control using Fuzzy logic

Finally, command u-phase voltages for each chopper cell, i.e., v_{ju}^* , are given as follows

$$v_{ju}^* = v_a^* + v_{Bju}^* - \frac{v_u^* + v_{com}^*}{4} + \frac{v_{dc}}{8} \quad (j = 1 - 4) \tag{5}$$

$$v_{ju}^* = v_a^* + v_{Bju}^* + \frac{v_u^* + v_{com}^*}{4} + \frac{v_{dc}}{8} \quad (j = 5 - 8) \tag{6}$$

Here, v_a^* and v_{Bju}^* are used to regulate the mean dc voltage, v_{ju}^* is the command motor voltage given by Fig. 3 described in the later section, v_{com}^* is the command common-mode voltage, and v_{dc} is the dc-link voltage used as feedforward control. The command rms value of the common-mode voltage V_{com}^* should be set as high as possible to reduce the amplitude of each ac circulating current, because it is inversely proportional to V_{com} . Moreover, there is no relationship between common-mode voltage and power rating of the motor.

In a low-speed range of $f \leq 12$ Hz, the rms value of the common-mode voltage V_{com} and the ac circulating currents \tilde{i}_{Zuvw} are controlled actively to mitigate the ac voltage fluctuation of each dc-capacitor voltage [14]. When $f \geq 20$ Hz, neither V_{com} nor \tilde{i}_{Zuvw} is super imposed. During a frequency range of $12 \leq f \leq 20$ Hz, V_{com}^* and \tilde{i}_{Zuvw} decrease linearly in their amplitude. Note that the dc circulating current is used to regulate the mean dc voltage of each dc capacitor through all frequency range [10].

III. MOTOR-SPEED CONTROL

This section describes a motor-speed control forming a feedback loop of three-phase stator currents for achieving a stable start-up of an induction motor. First, the motor-speed control is discussed in terms of a form and function. Second, it is compared with conventional motor-speed control techniques, i.e., “volts-per-hertz” and “slip-frequency” control techniques.

A. Control Principles

The motor-speed control forms a feedback loop of three phase stator currents to realize a stable start-up from standstill. This requires the current sensors attached to the ac terminals. The stator current in one phase is calculated by the corresponding arm currents detected. Therefore, no additional current sensor is required. Fig. 3 shows the block diagram for the motor-speed control. The three-phase stator currents are transformed into dc

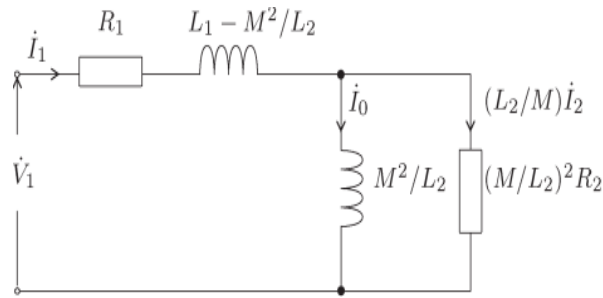


Fig. 4. Per-phase equivalent circuit based on the total linkage flux of the secondary windings

Per-phase equivalent circuit based on the total linkage flux of the secondary windings

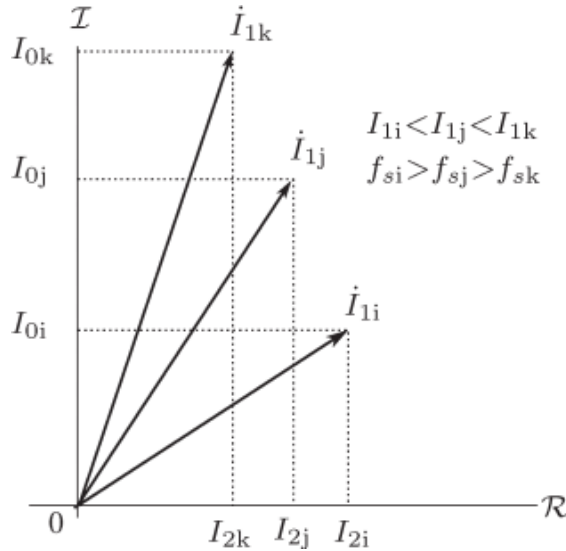


Fig.5. Phasor diagram for the stator currents with different amplitudes but the same torque

quantities by using the d-q transformation to enhance current controllability. In Fig. 5, θ^* is the phase information used for the d-q transformation, whereas i^*_d and i^*_q are the command currents given by

$$i^*_d = i^*_q = \sqrt{\frac{3}{2}} I^*_1 \tag{7}$$

Where I^*_1 is the command for the stator rms current. Note that I^*_1 and f^* are given not by feedback control, but by feed forward control, as described later. Fig.5.4 shows a per-phase equivalent circuit of an induction motor based on the total linkage flux of the secondary windings. Although this circuit is valid only under steady-state conditions, it is applicable to a fan- or blower-like load, in which the motor mechanical speed is adjusted slow enough to be considered as the steady-state condition. Here, i_1 is the phasor stator current, i_0 is the phasor magnetizing current, and i_2 is the phasor torque current. Note that i_0 and i_2 are orthogonal to each other in steady-state conditions. The rms value of i_1 , I_1 is given in as follows:

$$I_1 = \sqrt{I_0^2 + \left(\frac{L_2}{M} I_2\right)^2} \tag{8}$$

The motor torque T_M is expressed by using I_0 and I_2 that are the rms values of i_0 and i_2 , respectively, as follows :

$$T_M = 3PM I_0 I_2 \tag{9}$$

Where P is the pole-pair number. Fig. 5 shows a phasor diagram for three different phasor stator currents i_{1i} , i_{1j} , and i_{1k} but with producing the same torque, in which a relation of $I_{1i} < I_{1j} < I_{1k}$ holds. The imaginary flame I corresponds to the magnetizing current i_0 , and the real flame R corresponds to the torque current i_2 . It is obvious in (9) and Fig. 5 that the motor torque T_M is proportional to the area of the triangle surrounded by i_1, i_2 , and i_0 . The motor-speed control has no capability to control the magnetizing current and the torque current independently. However, when the phasor stator current changes from i_{1i} to i_{1j} , the torque current decreases from I_{2i} to I_{2j} and the magnetizing current increases from I_{0i} to I_{0j} , respectively, to keep the area of the

triangle constant. In other words, both I_0 and I_2 would change each of the amplitude automatically when I_1 changes. The slip frequency f_s is described by using I_2 and I_0 as follows:

$$F_s = \frac{R_2 I_2}{2\pi M I_0} \quad (10)$$

A relation of $f_{s1} > f_{sj} > f_{sk}$ exists in Fig.5.5, which are the slip frequencies at different operating points. The slip frequency has no freedom when T_M and I_1 are given.

B. Comparisons of Three Motor-Speed Control Techniques

Table I summarizes comparisons among the three motor speed control techniques, with a focus on similarity and difference. The “volts-per-hertz” control or shortly “V/f” control has two independent variables V_1 and f , in which V_1 is the stator voltage and f is the stator frequency. On the other hand, the two dependent variables are the stator current I_1 and the slip frequency f_s . The V/f control is a straight forward speed control requiring no speed sensor, which is based on feed forward control of V_1 and f . However, both motor and DSCC may suffer from an over current during the start-up or when a rapid change in torque occurs. The slip-frequency control has two independent variables I_1 and f_s , and the two dependent variables are V_1 and f . Here, the commands for I_1 and f_s are determined by a feedback loop of the motor mechanical speed, thus requiring a speed sensor attached to the motor shaft. The slip- frequency control can provide a faster torque response than the V/f control because of the existence of a feedback control for the motor mechanical speed.

The motor-speed control proposed for the DSCC-based induction motor drive has two independent variables I_1 and f , and the two dependent variables are V_1 and f_s . Unlike the slip frequency control, the motor-speed control requires no speed sensor because the commands for I_1 and f , i.e., I_1^* and f^* , are given not by feedback control, but by feedforward control, as done in the V/f control. This implies that the motor speed control proposed in this paper is inferior to the slip frequency control, in terms of torque controllability. However, it is applicable to a fan- or blower-like load, where the load torque is changing relatively slow and predictable. Moreover, no over current occurs during the start-up, or when a rapid change in torque occurs, because of the existence of a feedback control loop of the stator current.

TABLE 3.1 COMPARISONS AMONG EXISTING VOLTS-PER-HERTZ AND SLIP- FREQUENCY CONTROL TECHNIQUES AND THE PROPOSED MOTOR-SPEED CONTROL TECHNIQUE

	Volts-per-hertz control	Slip-frequency control	Proposed motor-speed control
Independent variables	V_1 and f	I_1 and f_s	I_1 and f
Dependent variables	I_1 and f_s	V_1 and f	V_1 and f_s
Voltage control	Feedforward	-	-
Current control	-	Feedback	Feedback
Speed sensor	No	Yes	No

An energy saving during a start-up does not make a significant contribution to total energy saving performance from a practical point of view because the motor power in a low speed range is negligible in applications such as fan- or blower-like loads. This means that a comparison of the three methods, in terms of energy saving performance during a start-up, does not make sense when fan- or blower-like loads are considered. Moreover, current stresses of the conventional motor-speed control techniques, the V/f and slip-frequency control, and the proposed motor- speed control technique are the same, at least, in a steady-state condition when a magnetizing current is set to the same value in all speed range.

IV. COMMAND STATOR CURRENTS

This section describes how to determine the command of the stator rms current I_1^* and the stator current frequency f^* .

The following two methods can be used to determine I_1^* and f^* :

- Determination from the equivalent circuit shown in Fig. 4;

- Determination from experiments

Determination From the Equivalent Circuit Shown in Fig.4

When a speed-versus-load-torque characteristic is known, the equivalent circuit shown in Fig. 4 can be used to determine I^*1 and f^* , along with the motor parameters including the moment of load inertia. The motor torque should satisfy the following equation during the start-up:

$$T_M - T_L > (J_M + J_L) \frac{d\omega_{rm}}{dt} \quad (11)$$

Where T_L is the load torque, J_M is the moment of inertia of the motor, J_L is that of the load, and ω_{rm} is the mechanical angular velocity. The right-hand term on (11) corresponds to an acceleration torque for the start up. For making analysis simple and easy, the following reasonable approximations are made.

- The stator-current frequency agrees well with its command f^* (i.e., $f=f^*$).
- The slip frequency f_s is much smaller than f (i.e., $f_s \ll f$).
- The moment of inertia of the load J_L is much larger than that of the motor J_M (i.e., $J_M \ll J_L$).

These three assumptions are applicable to fan- or blower-like loads for the following reasons. The first assumption is valid because the motor frequency, or the motor mechanical speed, is adjusted slowly, e.g., spending a few or several minutes to complete its start-up procedure. The second assumption is reasonable for an induction motor. The third assumption is valid because J_L is typically 50–100 times larger than J_M [10]. Finally, (11) is simplified as follows:

$$T_M - T_L > J_L \frac{2\pi df^*}{P dt} \quad (12)$$

Where $\omega_{rm} = 2\pi f^*/P$. Equation (12) means that the acceleration torque is proportional to the slope of required for the motor start-up is $T_M = T_L$, when the term on the right-hand side in (12) is small enough to be negligible. In other words, the slope of f^* should be set to be as small as possible to reduce the acceleration torque. The motor torque T_M in Fig. 5 is proportional to the area surrounded by I_1 , I_2 , and I_0 . The stator rms current required to produce a motor torque gets the smallest when the following relation is met:

$$I_0 = \frac{L_2}{M} I_2 \quad (13)$$

$$I_2 = \sqrt{\frac{T_M}{3pL_2}} \quad (14)$$

Finally, I_1 is obtained by substituting (14) into (8) as follows:

$$I_1 = \sqrt{\frac{2L_2 T_M}{3PM^2}} \quad (15)$$

When a speed-versus-load-torque characteristic is unknown, the current command I^*1 should be determined experimentally as follows. The initial value of I^*1 is set to zero. Then, I^*1 is being increased gradually where the motor starts rotating up. This method is similar to a traditional V/f control, in terms of no use of motor parameters. It is difficult to apply the motor-speed control to an application where a rapid or unpredictable change in load torque may happen. The reason is that I^*1 and f^* are given by feedforward control with no capability of handling a rapid or unpredictable change in torque. However, the motor-speed control is applicable to a fan- or blower-like load, where the motor mechanical speed is adjusted slow, and the load torque of which is proportional to a square of the motor mechanical speed. In this case, I_1 should be given so that it is proportional to the command motor mechanical speed, as predicted from (15). In addition, I_1 is proportional to the stator-current frequency because the slip frequency f_s is typically negligible compared to the stator-current frequency ($f_s \ll f$). Finally, experimental adjustment of the slope of $I_1/f (= I^*1/f^*)$ is required to achieve the stable start-up. The so-called “torque boost” function at low speeds, which is used in the V/f control, is applicable to the motor-speed control.

V.FUZZY LOGIC CONTROLLER

In FLC, basic control action is determined by a set of linguistic rules. These rules are determined by the system. Since the numerical variables are converted into linguistic variables, mathematical modeling of the system is not required in FC. The FLC comprises of three parts: fuzzification , interference engine and defuzzification. The FC is characterized as i. seven fuzzy sets for each input and output. ii. Triangular membership functions for simplicity. iii. Fuzzification using continuous universe of discourse. iv. Implication using Mamdani’s, ‘min’ operator. v. Defuzzification using the height method. Fuzzification: Membership function values are assigned to the linguistic variables, using seven fuzzy subsets: NB (Negative Big), NM (Negative Medium), NS (Negative Small), ZE (Zero), PS (Positive Small), PM (Positive Medium), and PB (Positive Big). The partition of fuzzy subsets and the shape of membership CE(k) E(k) function adapt the shape up to appropriate system. The value of input error and change in error are normalized by an input scaling factor.

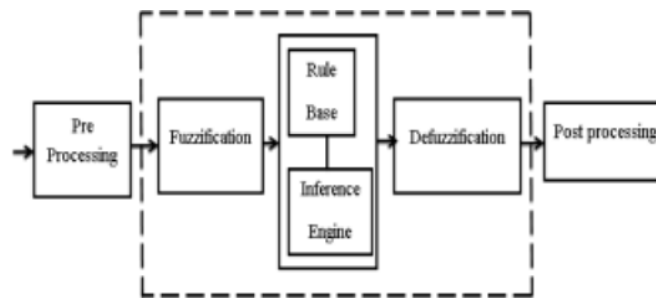


Fig.6. Fuzzy logic controller

Change in error	Error						
	NB	NM	NS	Z	PS	PM	PB
NB	PB	PB	PB	PM	PM	PS	Z
NM	PB	PB	PM	PM	PS	Z	Z
NS	PB	PM	PS	PS	Z	NM	NB
Z	PB	PM	PS	Z	NS	NM	NB
PS	PM	PS	Z	NS	NM	NB	NB
PM	PS	Z	NS	NM	NM	NB	NB
PB	Z	NS	NM	NM	NB	NB	NB

In this system the input scaling factor has been designed such that input values are between -1 and +1. The triangular shape of the membership function of this arrangement presumes that for any particular E(k) input there is only one dominant fuzzy subset. The input error for the FLC is given as

$$E(k) = \frac{P_{ph(k)} - P_{ph(k-1)}}{V_{ph(k)} - V_{ph(k-1)}}$$

$$CE(k) = E(k) - E(k-1)$$

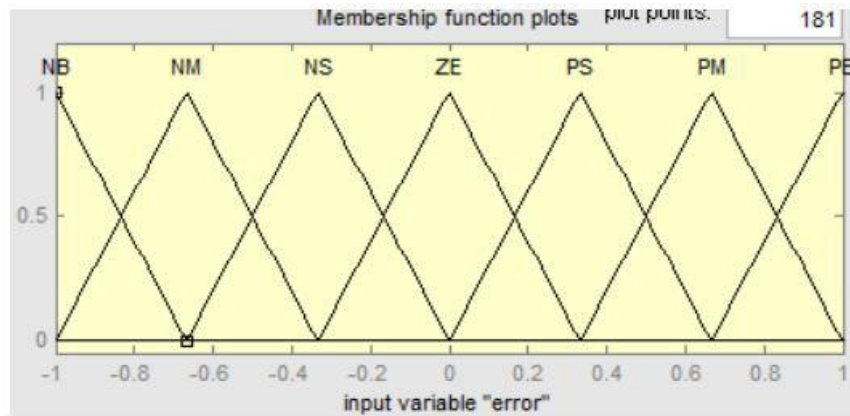


Fig.7.Membership functions

Inference Method: Several composition methods such as Max–Min and Max-Dot have been proposed in the literature. In this paper Min method is used. The output membership function of each rule is given by the minimum operator and maximum operator. Table 1 shows rule base of the FLC. Defuzzification: As a plant usually requires a nonfuzzy value of control, a defuzzification stage is needed. To compute the output of the FLC, height method is used and the FLC output modifies the control output. Further, the output of FLC controls the switch in the inverter. In UPQC, the active power, reactive power, terminal voltage of the line and capacitor voltage are required to be maintained. In order to control these parameters, they are sensed and compared with the reference values. To achieve this, the membership functions of FC are: error, change in error and output. The set of FC rules are derived from

$$u = -[\alpha E + (1-\alpha)C] \quad (15)$$

Where α is self-adjustable factor which can regulate the whole operation. E is the error of the system, C is the change in error and u is the control variable. A large value of error E indicates that given system is not in the balanced state. If the system is unbalanced, the controller should enlarge its control variables to balance the system as early as possible. On the other hand, small value of the error E indicates that the system is near to balanced state. Overshoot plays an important role in the system stability. Less overshoot is required for system stability and in restraining oscillations. During the process, it is assumed that neither the UPQC absorbs active power nor it supplies active power during normal conditions. So the active power flowing through the UPQC is assumed to be constant. The set of FC rules is made using Fig.(b) is given in Table 1.

VI. SIMULATION RESULTS

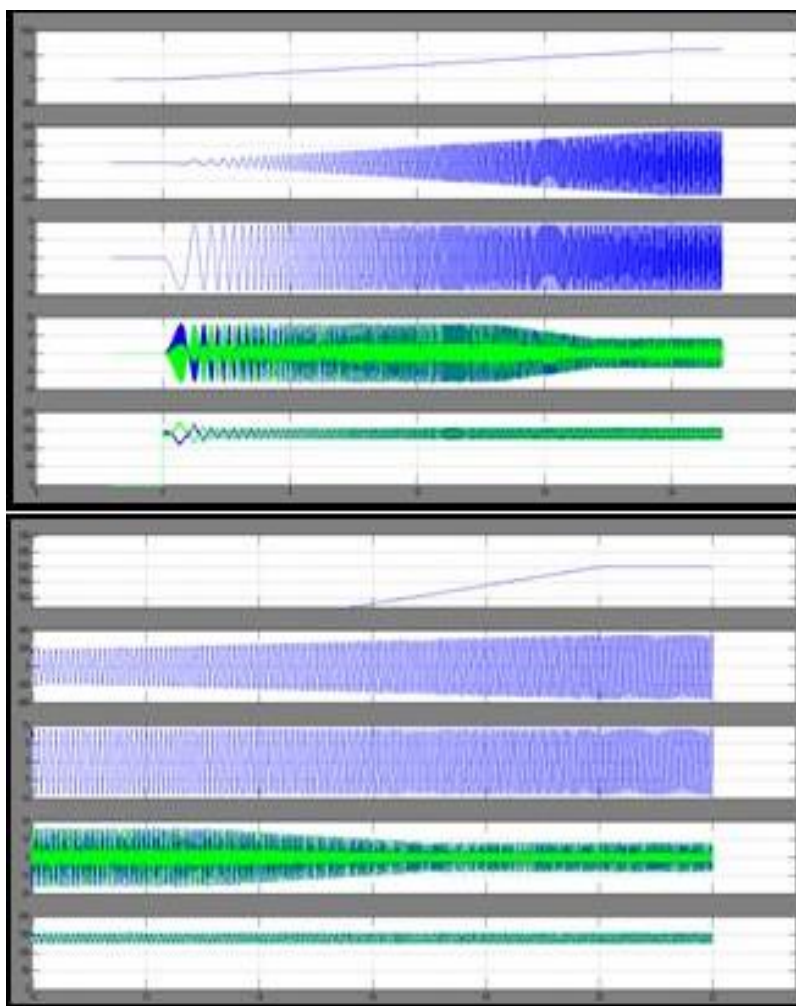


Fig.8. Simulation start-up waveforms when $I1^* = 6.4$ A (20%) and $TL = 0\%$, where $I0 = 6.4$ A (35%).

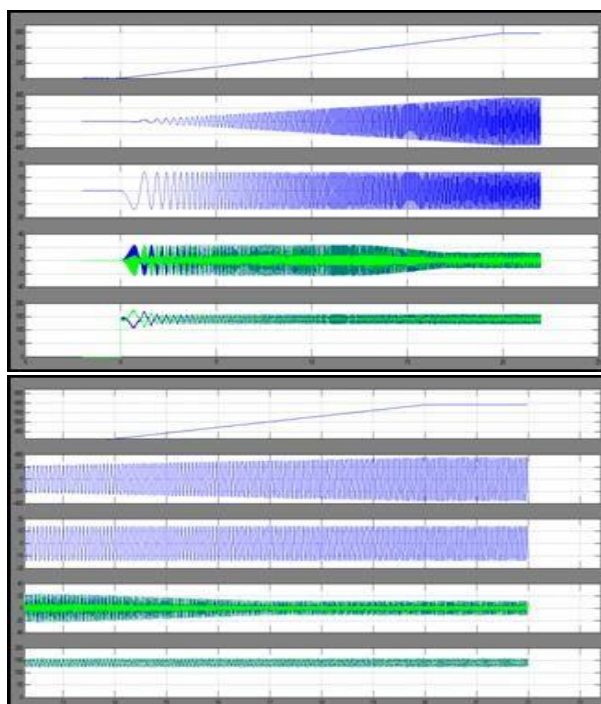


Fig.9 . Simulation start-up waveforms when $I1^* = 6.4$ A (20%) and $TL = 0\%$, where $I0 = 6.4$ A (35%).

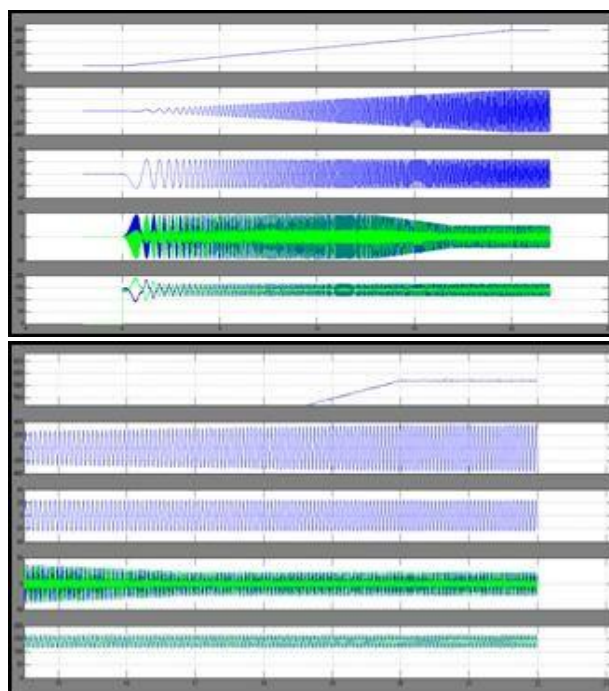


Fig.10. Simulation start-up waveforms when $I1^* = 14$ A (44%), and $TL = 40\%$, where $I0 = 9.9$ A (54%).

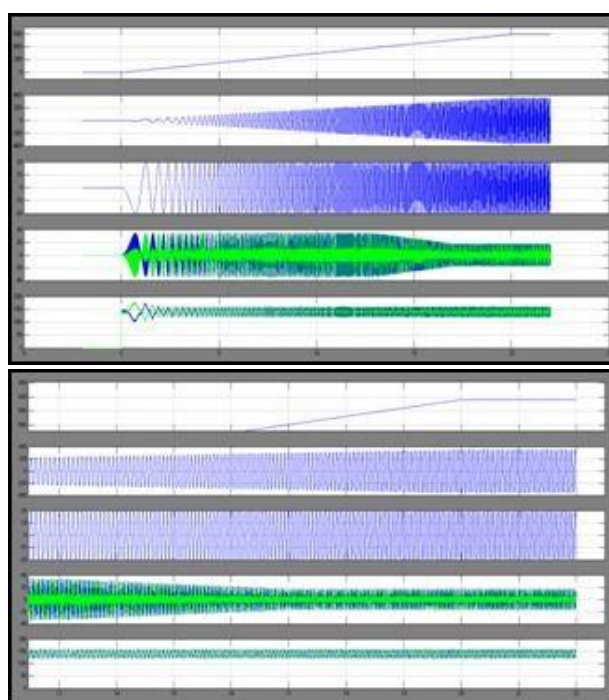


Fig.11. Simulation start-up waveforms when $I1^* = 17$ A (53%), and $TL = 60\%$, where $I0 = 12.0$ A (65%).

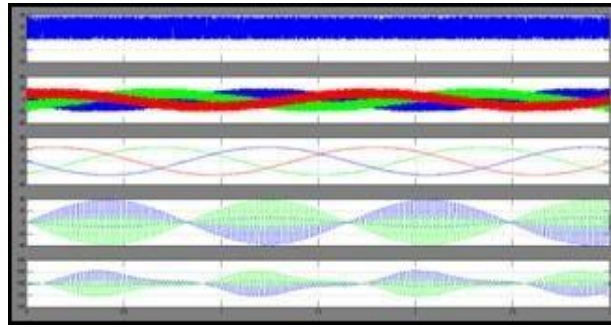


Fig.12. Simulation steady-state waveforms when $I_1^* = 17 \text{ A}$ (53%), $f^* = 1 \text{ Hz}$, and $TL = 60\%$, where $I_0 = 12.0 \text{ A}$ (65%).

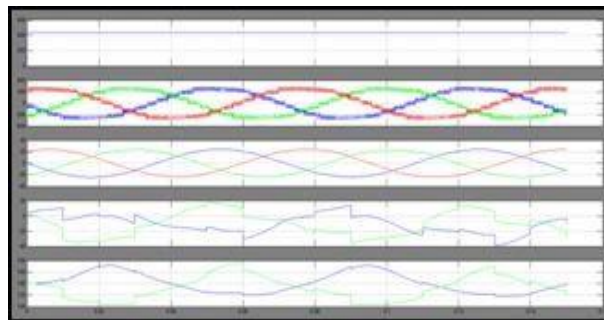


Fig. 13. Simulation steady-state waveforms when $I_1^* = 17 \text{ A}$ (53%), $f^* = 15 \text{ Hz}$, and $TL = 60\%$, where $I_0 = 12.0 \text{ A}$ (65%).

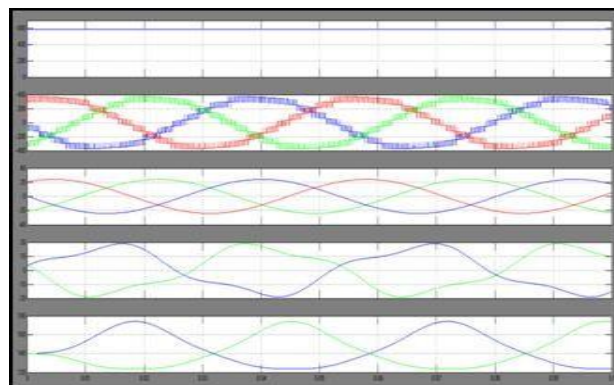


Fig.14. Simulation steady-state waveforms with $I_1^* = 17 \text{ A}$ (53%), $f^* = 20 \text{ Hz}$, and $TL = 60\%$, where $I_0 = 12.0 \text{ A}$ (65%).

VII. CONCLUSION

This paper has proposed a practical start-up method for DSCC-driven induction motor with no speed sensor from standstill to middle speed. This start-up method is characterized by combining capacitor voltage control and motor-speed control. The motor speed control with the minimal stator current under a load torque is based on the combination of feedback control of the three-phase stator currents with feed forward control of their amplitude and frequency. The arm-current amplitudes and ac-voltage fluctuations across each of the dc capacitors can be reduced to acceptable levels. Simulation results shown that the motor loaded with 60% can achieve a stable start up from standstill to a middle speed of $N_{rm} = 588 \text{ min}^{-1}$ without overvoltage and over current. The start-up torque has been increasing by a factor of three, without additional stress on both arm currents and ac-voltage fluctuations. This method is suitable particularly for adjustable-speed motor drives of large-capacity fans, blowers, and compressors for energy savings.

REFERENCES

- [1] P. W. Hammond, "A new approach to enhance power quality for medium voltage ac drives," *IEEE Trans. Ind. Appl.*, vol. 33, no. 1, pp. 202–208, Jan./Feb. 1997.
- [2] R. Teodorescu, F. Blaabjerg, J. K. Pedersen, E. Cengelci, and P. N. Enjeti, "Multilevel inverter by cascading industrial VSI," *IEEE Trans. Ind. Appl.*, vol. 49, no. 4, pp. 832–838, Jul./Aug. 2002.
- [3] J. Rodriguez, S. Bernet, J. O. Bin Wu, and S. Pontt, "Multilevel voltage source-converter topologies for industrial medium-voltage drives," *IEEE Trans. Ind. Electron.*, vol. 54, no. 6, pp. 2930–2945, Dec. 2007.
- [4] S. Malik and D. Kluge, "ACS 1000 world's first standard ac drive for medium-voltage applications," *ABB Rev.*, no. 2, pp. 4–11, 1998.
- [5] H. Akagi, "Classification, terminology, and application of the modular multilevel cascade converter (MMCC)," *IEEE Trans. Power Electron.*, vol. 26, no. 11, pp. 3119–3130, Nov. 2011.
- [6] A. Lesnicar and R. Marquardt, "An innovative modular multilevel converter topology suitable for a wide power range," in *Conf. Rec. IEEE Bologna Power Tech, 2003*, [CD-ROM].
- [7] M. Hagiwara and H. Akagi, "Control and experiment of pulse-width modulated modular multilevel converters," *IEEE Trans. Power Electron.*, vol. 24, no. 7, pp. 1737–1746, Jul. 2009.
- [8] M. Hiller, D. Krug, R. Sommer, and S. Rohner, "A new highly modular medium voltage converter topology for industrial drive applications," in *Conf. Rec. EPE, 2009*, pp. 1–10.
- [9] S. Rohner, J. Weber, and S. Bernet, "Continuous model of modular multilevel converter with experimental verification," in *Conf. Rec. IEEE ECCE, 2011*, pp. 4021–4028.
- [10] M. Hagiwara, K. Nishimura, and H. Akagi, "A medium-voltage motor drive with a modular multilevel PWM inverter," *IEEE Trans. Power Electron.*, vol. 25, no. 7, pp. 1786–1799, Jul. 2010.
- [11] A. Antonopoulos, L. Angquist, S. Norrga, K. LIVES, and H. P. Nee, "Modular multilevel converter ac motor drives with constant torque from zero to nominal speed," in *Conf. Rec. IEEE-ECCE, 2012*, pp. 739–746.
- [12] J. Kolb, F. Kammerer, and M. Braun, "Dimensioning and design of a modular multilevel converter for drive applications," in *Conf. Rec. EPE, 2012*, pp. LS1a-1.1-1–LS1a-1.1-8, [CD-ROM].
- [13] A. J. Korn, M. Winkelnkemper, and P. Steimer, "Low output frequency operation of the modular multilevel converter," in *Conf. Rec. IEEE-ECCE, 2010*, pp. 3993–3997.
- [14] M. Hagiwara, I. Hasegawa, and H. Akagi, "Startup and low-speed operation of an adjustable speed motor driven by a modular multilevel Cascade inverter (MMCI)," *IEEE Trans. Ind. Appl.*, vol. 49, no. 4, pp. 1556–1565, Jul./Aug. 2013.
- [15] J. Holtz, "Sensorless control of induction motor drives," *Proc. IEEE*, vol. 90, no. 8, pp. 1359–1394, Aug. 2002.
- [16] R. J. Pottebaum, "Optimal characteristics of a variable-frequency centrifugal pump motor drive," *IEEE Trans. Ind. Appl.*, vol. 20, no. 1, pp. 23–31, Jan. 1984.
- [17] N. Hirotsu, H. Akagi, I. Takahashi, and A. Nabae, "A new equivalent circuit of induction motor based on the total linkage flux of the secondary windings," *Elect. Eng. Japan*, vol. 103, no. 2, pp. 68–73, Mar./Apr. 1983.
- [18] A. Munoz-Garcia, T. A. Lipo, and D. W. Novotny, "A new induction motor V/f control method capable of high-performance regulation at low speeds," *IEEE Trans. Ind. Appl.*, vol. 34, no. 4, pp. 813–821, Jul./Aug. 1998.
- [19] H. Fujita, S. Tominaga, and H. Akagi, "Analysis and design of a dc voltage-controlled static var compensator using quad-series voltage source inverters," *IEEE Trans. Ind. Appl.*, vol. 32, no. 4, pp. 970–977, Jul./Aug. 1996.
- [20] H. Peng, M. Hagiwara, and H. Akagi, "Modeling and analysis of switching-ripple voltage on the dc link between a diode rectifier and a modular multilevel cascade inverter (MMCI)," *IEEE Trans. Power Electron.*, vol. 28, no. 1, pp. 75–84, Jan. 2013.